Stem Cell Reports, Volume *13*

Supplemental Information

Stem Cell Modeling of Neuroferritinopathy Reveals Iron as a Determinant of Senescence and Ferroptosis during Neuronal Aging

Anna Cozzi, Daniel I. Orellana, Paolo Santambrogio, Alicia Rubio, Cinzia Cancellieri, Serena Giannelli, Maddalena Ripamonti, Stefano Taverna, Giulia Di Lullo, Ermanna Rovida, Maurizio Ferrari, Gian Luca Forni, Chiara Fiorillo, Vania Broccoli, and Sonia Levi

SUPPLEMENTAL INFORMATION

Stem Cell Modelling of Neuroferritinopathy Reveals Iron as a Determinant of Senescence and Ferroptosis During Neuronal Ageing.

Anna Cozzi[1], Daniel I. Orellana[1], Paolo Santambrogio[1], Alicia Rubio[2,3], Cinzia Cancellieri[2], Serena Giannelli[2], Maddalena Ripamonti[4], Stefano Taverna[4], Giulia Di Lullo[5], Ermanna Rovida[6], Maurizio Ferrari[7,8], Gian Luca Forni[9], Chiara Fiorillo[10], Vania Broccoli[2,3,] and Sonia Levi[1,8*]

Inventory of Supplemental Information

- Figure S1 with Legend
- Figure S2 with Legend
- Figure S3 with Legend
- Figure S4 with Legend
- Figure S5 with Legend
- Table S1
- Table S2
- Table S3

Supplemental Figures and legends

Figure S1

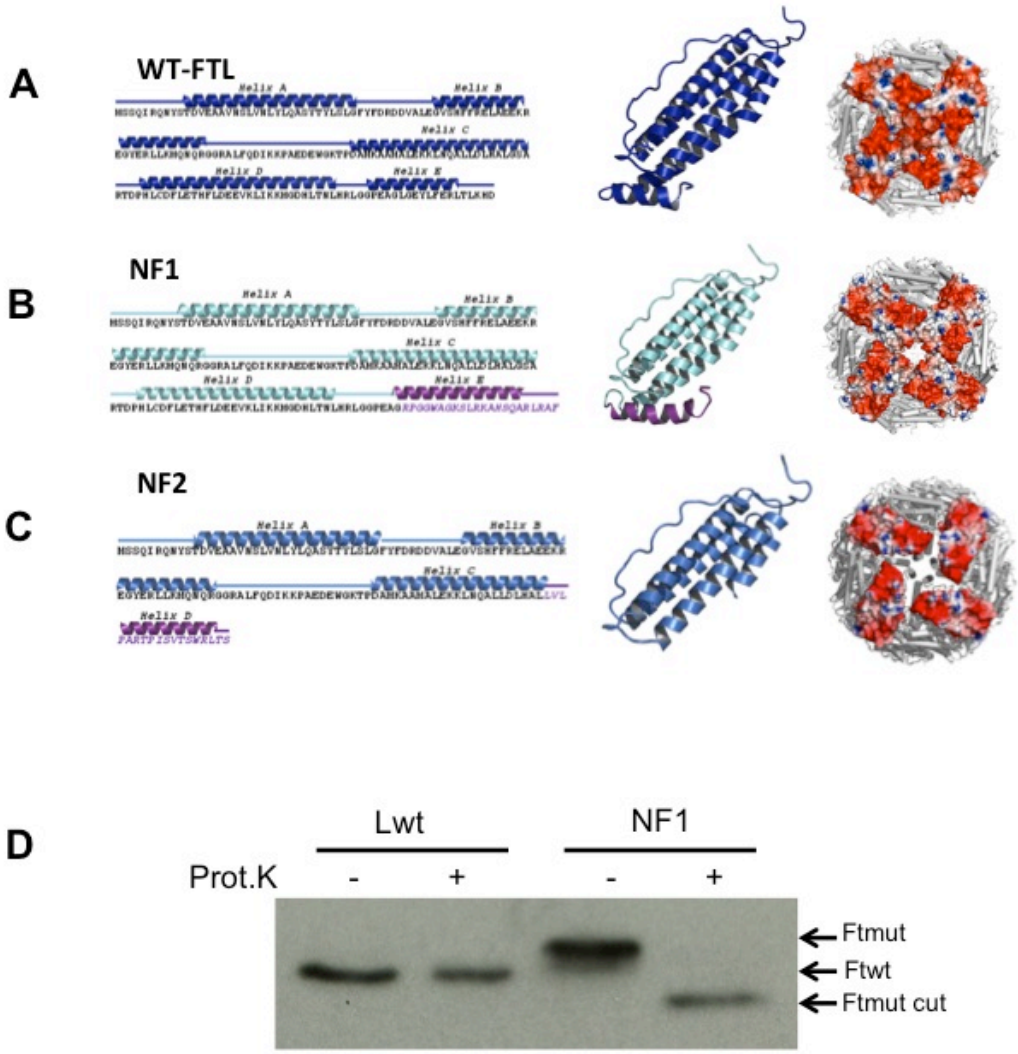

Figure S1. Mutant ferritin alterations. Related to section results "Development and characterization of NF fibroblasts and iPSC-derived neuronal models" and "NF fibroblasts/iPSC-derived NPCs and neurons showed cellular iron mobilization and ferritin/iron aggregates "

Sequence and structural features of NF1 and NF2 mutants compared to those of the wild type L-ferritin. Left side: Secondary structure elements are depicted in correspondence with the sequences.

(A) In the wild type (dark blue), the secondary structure information is obtained by the X-ray coordinates of PDB: 2FFX.

(B) In the mutants NF1 (cyan) and (C) NF2 (light blue), the secondary structure prediction is obtained with the Psi-pred tool. Purple regions in NF1 and NF2 correspond to the mutated sequence portions. Central: Tertiary structure of ferritin subunits; WT-FTL is derived from the X-ray structure; NF1 and NF2 are molecular models obtained by the threading approach. Right side: 3D representation of the fully assembled ferritin 24 mer viewed from the four-fold symmetry axes. Subunits forming the four-fold channel are depicted with a representation of

the surface electrostatic potential to show the modification in the charge distribution arrangement in NF1 and NF2 compared to that in WT-FTL.
(D) NF1 variant protein (Ftmut) and L-ferritin wild type (Ftwt) were expressed in HeLa cells in the soluble form; 20 mg of both soluble cell homogenates were incubated with or without Proteinase K (Prot.K), separated on 12% SDS-PAGE, blotted, and incubated with an anti-human L-ferritin antibody

Figure S2

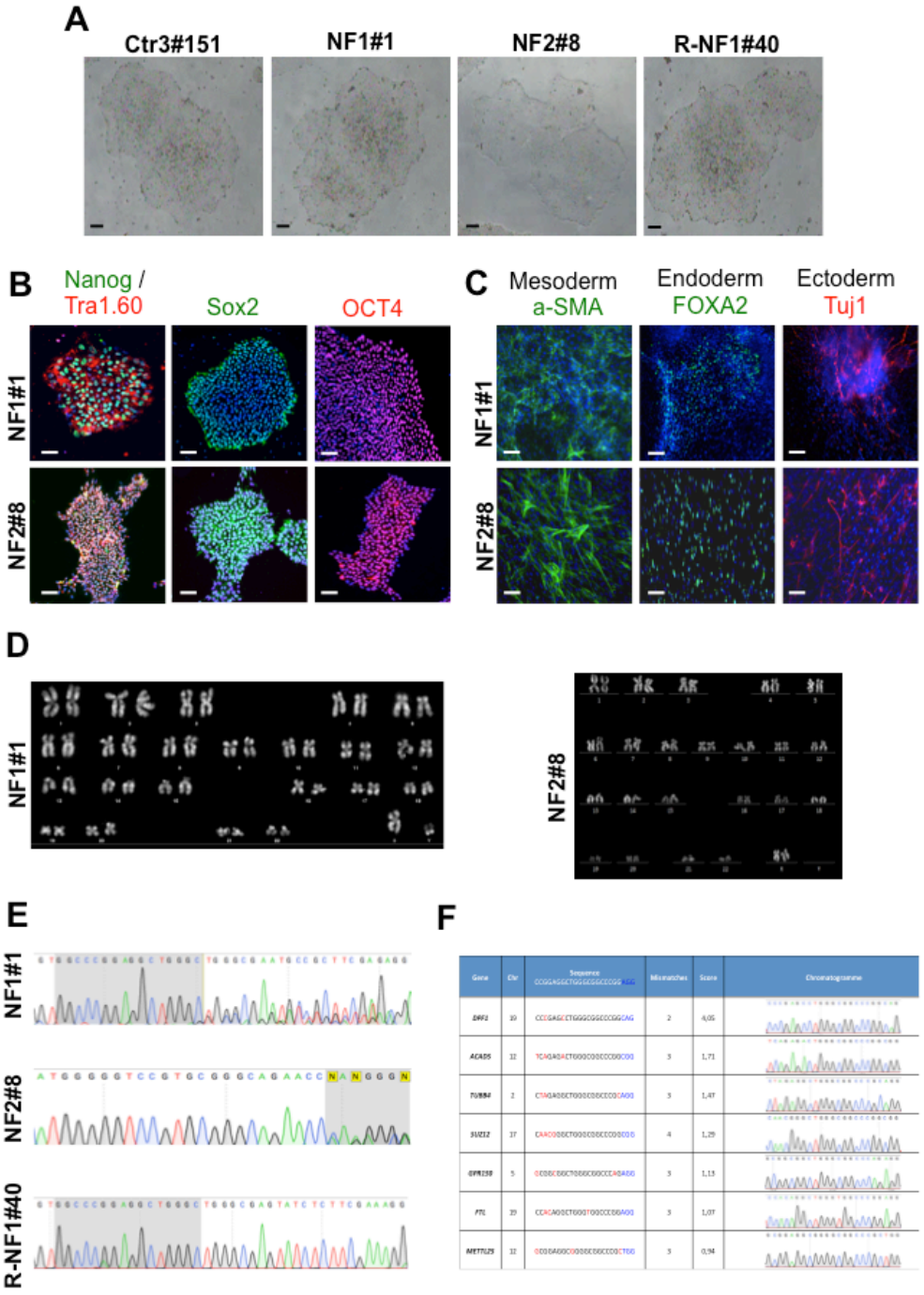

Figure S2. Characterization of iPSC clones. Related to section results "Development and characterization of NF fibroblasts and iPSC-derived neuronal models" and "NF fibroblasts/iPSC-derived NPCs and neurons showed cellular iron mobilization and ferritin/iron aggregates "

(A) Representative images in bright field of feeder free iPSC colonies generated from each subject. Cells form large iPSC colonies containing tightly packed cells with distinct borders. Scale bar 100 μm

(B) The stem cell pluripotency features were fully characterized by an immunofluorescence analysis. Representative images of NF1 and NF2 iPSC colonies immunostained for the markers Nanog, Tra-1-60, Sox2, and OCT4. Scale bar 100 μm.
(C) Representative IF image of NF1 and NF2 iPSCs differentiated *in vitro* into all three germ layers (endoderm, FoxA2; mesoderm, SMA; and ectoderm, Tuj1). Hoechst dye was used to stain the nuclei. Scale bar 20 μm.
(D) The selected iPSCs of NF1 and NF2 were assessed for the correct karyotype.
(E) DNA sequence analysis of iPSC clones NF1 and NF2 confirming the presence of the indicated mutation in *FTL1* (469_484dup and 351delG_InsTTT, respectively). The sequences showed the presence of both the mutated and wild type alleles in NF1 and NF2.
The isogenic control cells (R-NF1), was obtained restoring the wild type DNA sequences of *FTL1* by CRISPR/Cas9 technology, using a single-stranded oligodeoxynucleotide (ssODN) donor template and an sgRNA, (Supplementary Table 2) directed specifically to the mutated allele of one iPSC clone (number 7) carrying the 469_484dup mutation. DNA sequence analysis of the CRISPR/Cas9 clone confirmed the correction of the mutation in the *FTL1* gene.
(F) Analysis of the 7 most likely off-target genomic sites with less than 5 mismatches, as predicted by the CRISPR Design Tool, in the R-NF1 clone. In the sequences (5´-3´), the PAM domains are highlighted in blue, and the nucleotide mismatches with respect to the sgRNA sequence are highlighted in red. No alterations were detected in the sequences of the 7 genes studied

Figure S3

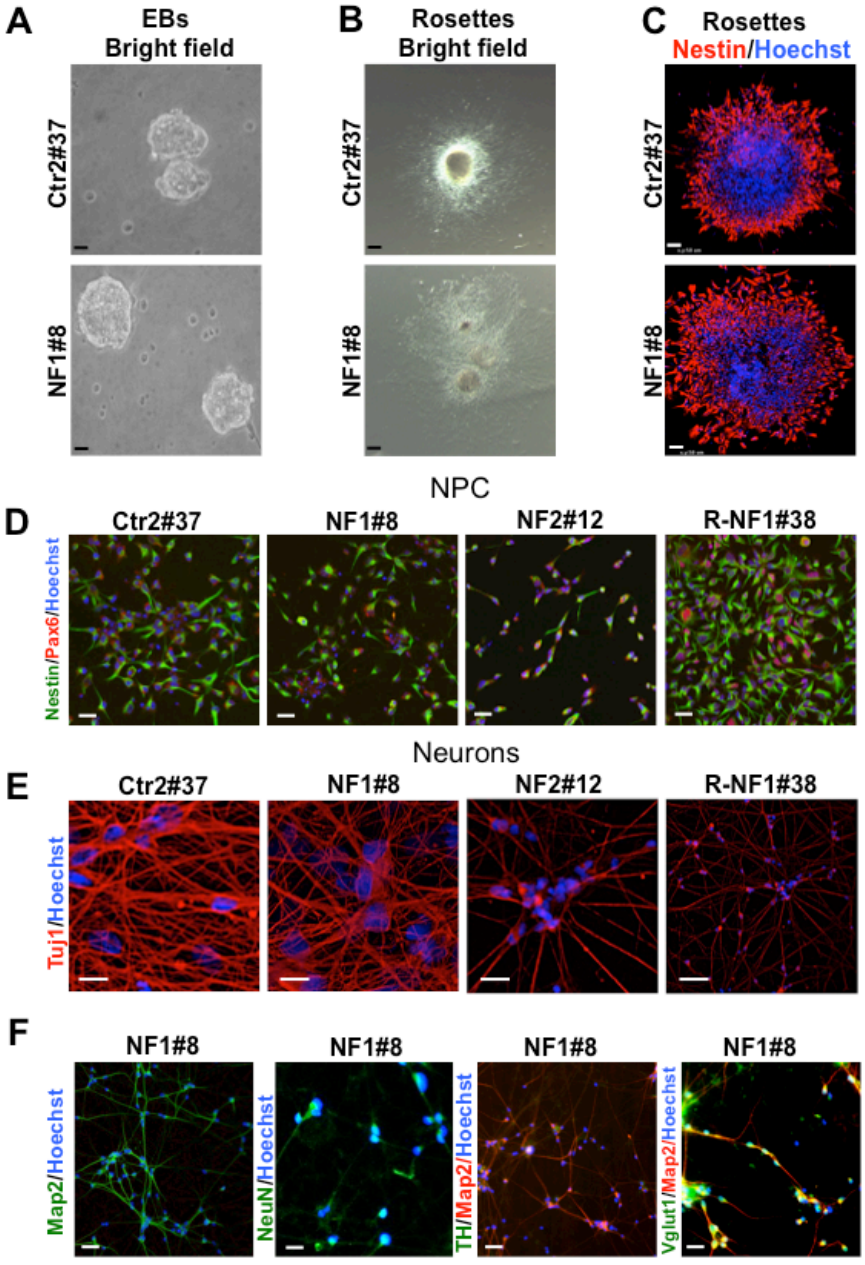

Figure S3 Characterization of EB, NPC and derived neurons. Related to section results "Development and characterization of NF fibroblasts and iPSC-derived neuronal models" and "NF fibroblasts/iPSC-derived NPCs and neurons showed cellular iron mobilization and ferritin/iron aggregates "

(A) Representative bright field images of control and patient NF1 EBs obtained from feeder free iPSC colonies. Cells grown in suspension forming packed cell bodies. Scale bar 50 μm

(B) Representatives images in bright field of a control and patient NF1. EBs were able to form rosettes when grown on Matrigel. Scale bar 50 μm

(C) Representative immunostaining of control and NF1 patient rosettes positive for Nestin. Scale bar 50 μm.

(D) The neural rosettes were isolated, disaggregated, and transferred to N2/B27-based medium supplemented with the growth factor FGF2 (Marchetto et al., 2010). Under these conditions, the NPCs gave rise to long-term expandable populations of highly proliferative cells. Stable NPC cultures were established with equal efficiency from all controls and NF-iPSCs. Representative images of NPCs obtained from neural rosettes differentiated from controls, NF patients and R-NF1. NPCs express the markers Nestin and Pax6.
(E) The cells were transduced with a lentivirus overexpressing the neurogenin-2 (Ngn2) neurogenic factor and puromycin resistance (Orellana et al., 2016). Representative images from control, NF1, NF2 and R-NF1 positive for the neuronal marker bIII-tubulin (Tuj1).
(F) One representative experiment on patient NF1 showing positivity for the neuronal markers Map2, NeuN, TH and Vglut1. For all immunostaining shown Hoechst dye was used to stain the nuclei.
Scale bars in D-F 20 μm

Figure S4

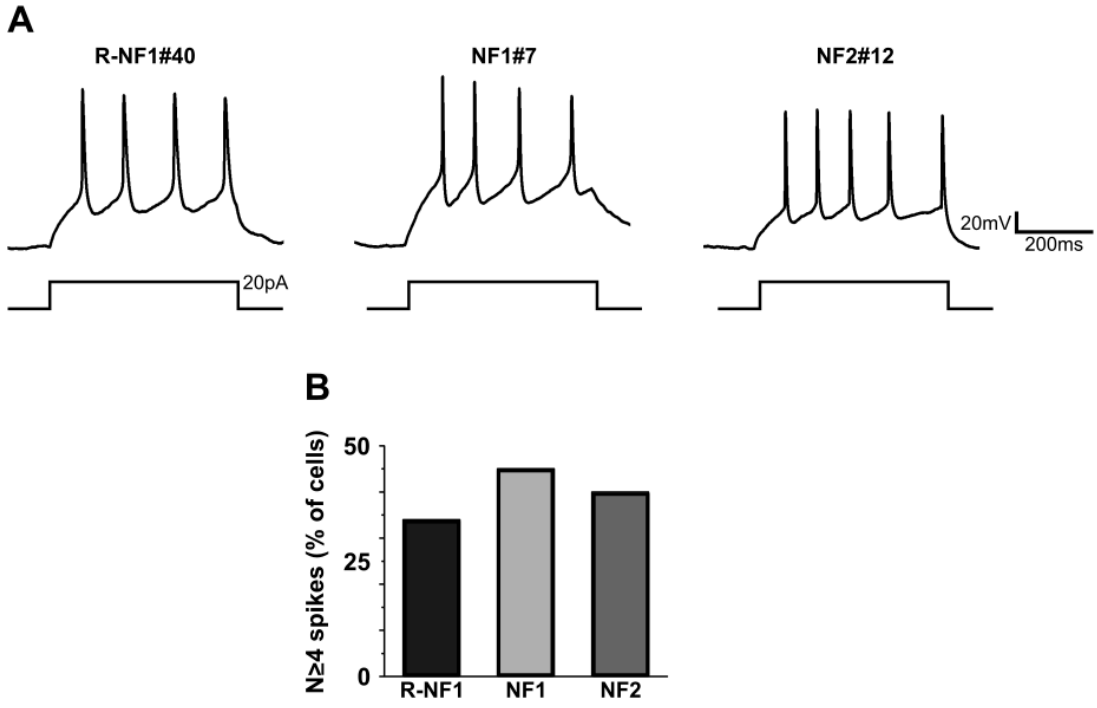

Figure S4. Electrophysiological profile of iPSC-derived neurons.
(A) Examples of evoked action potential firing activity in individual neurons collected from two different patients (NF1 and NF2) and an isogenic control (R-NF1); lower traces represent the injected depolarizing current steps and relative amplitudes.
(B) The mean percentage of cells able to fire ≥4 action potentials in response to suprathreshold stimuli (400ms). Recording from 4 experiments were pooled. NF1 e NF2 did not significantly differ from the R-NF1 (R-NF1: 12 viable cells of 35, 34%; NF1: 9/20, 45%; NF2: 8/20, 40%). These data confirm the proper electrical functionality of our iPSC-derived neurons and suggest that NF neurons do not display overtly aberrant electrophysiological properties.

Figure S5

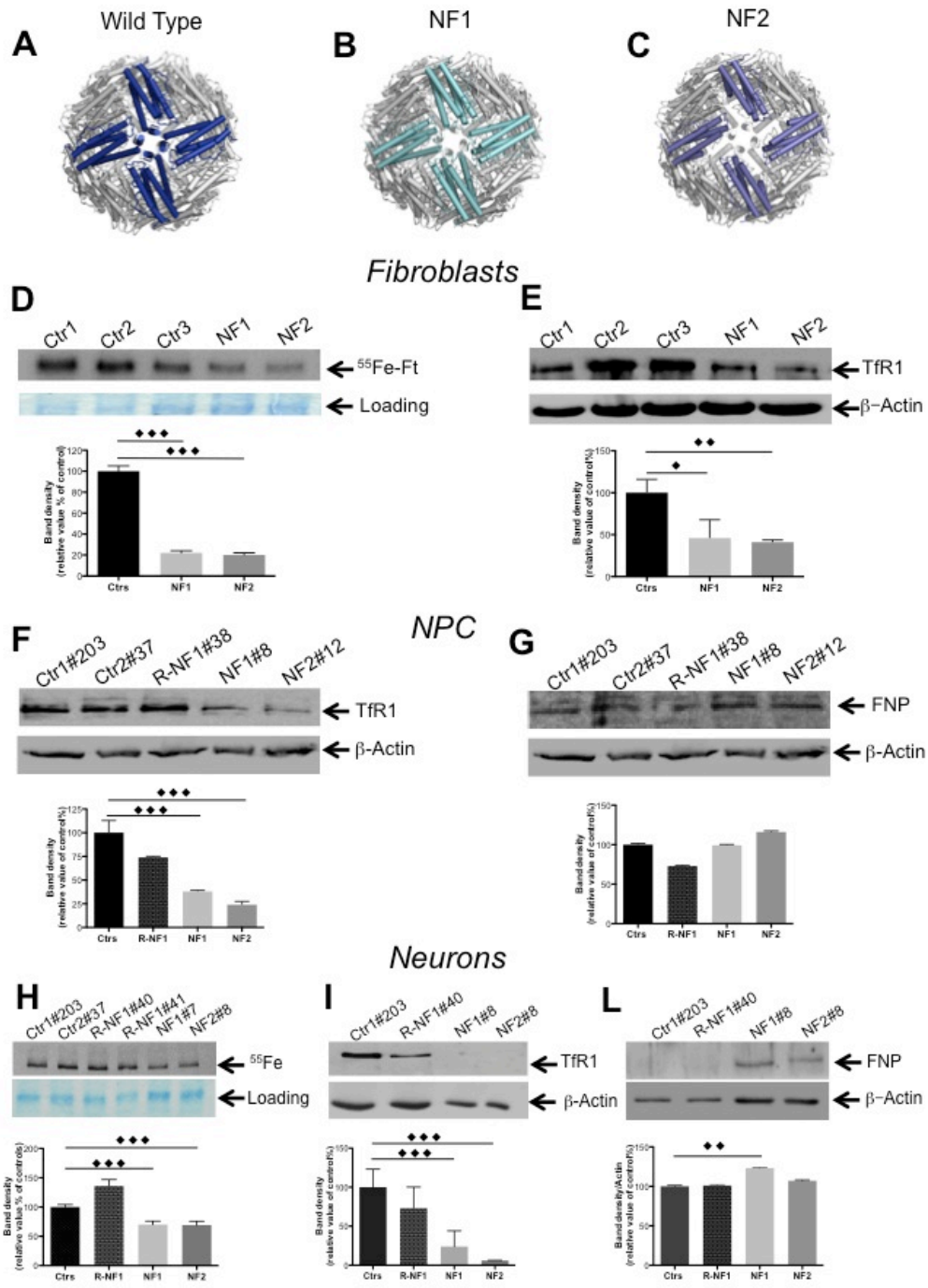

Figure S5. NF fibroblasts/iPSC-derived NPCs and neurons showed cellular iron mobilization due to ferritin alteration. Related to section results "Development and characterization of NF fibroblasts and iPSC-derived neuronal models" and "NF fibroblasts/iPSC-derived NPCs and neurons showed cellular iron mobilization and ferritin/iron aggregates "

(A) Cartoon representation of the 24 subunits assembled form of L ferritins. Human wild type L-ferritin homopolymer from the X-ray structure PDB: 2FFX; the subunits shown in blue highlight the four-fold symmetry axis lined by the C-terminal helices (helix-E) narrowing the channel width. (B**)** Computer simulation of the four-fold channel formed by the NF1 (cyan) and **(**C**)** NF2 (light blue) mutated subunits replacing the wt (blue) shown in panel (A). The 3D structure of the mutants was obtained by computer modelling using the programme Threader.

The placement of the 4 mutated subunits to form the channel is only hypothetical and is presented to emphasize the dramatic effect of both mutations on the channel geometry, leading to a larger opening that likely impairs the ability to regulate the iron storage inside the ferritin cavity.

(D) Control and patient fibroblasts were incubated for 18 h with 2 μCi/ml of ^{55}FeAC. Soluble homogenate proteins (10 μg) were loaded on 7% non-denaturing PAGE, exposed to autoradiography and evaluated by densitometry. Coomassie blue staining of total protein as a loading control. The results are expressed as the mean +/- SD relative to the controls of three independent experiments. The arrows indicate ferritin mobility or loading.

(E) Soluble homogenate proteins (20 μg) from fibroblasts were separated on 12% SDS-PAGE, blotted, and incubated with an anti-human TfR1 antibody.

(F) TfR1 in soluble homogenate proteins (20 μg) from NPCs.

(G) FPN in soluble homogenate proteins (20 μg) from NPCs.

The incubation with the anti-β actin antibody was performed as a loading control. Quantification was performed by densitometry.

The results are presented as the mean +/- SD of three independent experiments.

(H) Control and patient neurons treated as described in (D).

(I) TfR1 in neurons soluble homogenates.

(L**)** FPN in neurons soluble homogenates.

Quantification was performed by densitometry. The results are presented as the mean +/- SD of three independent experiments.

All the data were analysed by unpaired, two-tailed t-test, *$p<0.05$, **$p<0.01$, ***$p<0.001$.

Supplemental Tables

Table S1. Ferritin content

Sample	FtL (ng/mg proteins)	FtH (ng/mg proteins)
Ctr1	17 ± 2.1	99 ± 9.5
Ctr2	18 ± 2.5	96 ± 5.5
Ctr3	19 ± 7.2	110 ± 16.1
NF1	49 ± 9.1	180 ± 15.2
NF2	16.4 ± 5.1	281 ± 1

Extracts from healthy control and patient fibroblasts were analysed for ferritin content using ELISAs specific for H-and L-ferritins. The values are presented as the means +/-SD of three independent experiments performed in triplicate.

Table S2. Primers sets used in the experiments.

Name	Sequence 5'-3'
P1 Fw	CAACTGGCTGCTCTCTCCCC
P1 Re	ACAGCCAGGCAAGCAGAGAA
P2 Fw	CAGGGTGCGGAGAGTGATAA
P2 Re	CCAGGAAGTCACAGAGCTGA
ssODN	AAGTGAAGCTTATCAAGAAGATGGGTGACCACCTGACCAACCTCCAC AGGCTGGGTGGCCCGGAGGCTGGGCTGGGCGAGTATCTCTTCGAAA GGCTCACTCTCAAGCACGACTAAGAGC
sgRNA	CCGGAGGCTGGGCGGCCCGGAGG
DPF1 Fw	GGGCCTGTTTGAGTCCCAGT
DPF1 Re	GTAAATCTGTCCCGGGGCCA
ACADS Fw	TGACAGAGATGCCGGCAGAG
ACADS Re	CGGGAGGACAACTGAGGTGT
TUBB4 Fw	CGCGACTCTTAATCCCAGCG
TUBB4 Re	TCGGCCAAAGTCACCAGGAG
SUZ12 Fw	GACTCGCTAAACCGCTCGCT
SUZ12 Re	GGGAAGGAGGAGAGAGGGGA
GPR150 Fw	TAGCCCCTCAATTCTGCCGC
GPR150 Re	CTGGCTGCAGGGACGTTGG
FTL2 Fw	TCTATGTGCCGAGTGTGTGT
FTL2 Re	CTATTGGCTGGAGGGAGAGG
METTL25 Fw	TGGAAGCCAGCAGAACCAGG
METTL25 Re	TAGAGCCAAGCCTAGCCTGC
SLC7A11 Fw	TCCTGCTTTGGCTCCATGAACG
SLC7A11 Re	AGAGGAGTGTGCTTGCGGACAT
NCOA4	Cat. no PPH02290A Qiagen

Table S3. Antibodies used in the study.

Antibody-Species	Manufacturer	Catalogue No	Application	Dilution
Oct4 – Rb	Abcam	AB18976	IF	1:250
NANOG – Rb	Abcam	AB21603	IF	1:250
TRA-1-60 – Ms	Millipore	MAB4350	IF	1:250
SOX2 – Rb	Abcam	AB59776	IF	1:250
FoxA2 – Rb	Abcam	AB40874	IF	1:250
Anti-SMA – Ms	Sigma-Aldrich	A2547	IF	1:500
βIII-tubulin/Tuj1 – Ms	Covance	MMS435P100	IF	1:500
βIII-tubulin/Tuj1 – Rb	Covance	PRB435P100	IF	1:500
Anti-human Nestin – Ms	Millipore	MAB5326	IF	1:500
Alexa 647 anti-human CD56 (NCAM) – Ms	BD Biosciences	557711	IF	1:80
Pax6 – Rb	Covance	PRB278P	IF	1:200
TH – Rb	Covance	AB10312	IF	1:200
NeuN – Ms	Millipore	MAB377	IF	1:200
Vglut1 – Gp	Synaptic	135304	IF	1:200
p53-Ms	Santa Cruz Biot.	Sc-126	IF	1:200
NCOA4-Rb	Santa Cruz Biot	Sc-28749	IF/WB	1:200/1:400
TfR1 – Ms	Zymed laboratories	13-6800	WB	1:2000
FtH-Ms	Home made	Luzzago et al. (1986)	IF/ELISA	5-10mg/ml
FTL-Ms	Home made	Luzzago et al (1986)	ELISA	10 mg/ml
FPN-Rb	Alpha Diagn. Int.	MTP11-S	WB	1:1000
Actin – Ms	Sigma-Aldrich	A5441	WB	1:6000
p62-Ms	Santa-Cruz	Sc-28359	WB	1/500
LC3-Rb	Sigma-Aldrich	L8918	WB	1/1000
Anti-mouse HRP	Sigma-Aldrich	AP130P	WB	1:100000
Anti-rabbit HRP	Sigma-Aldrich	AP156P	WB	1:50000
Anti-mouse-546	Imm. Sciences	IS20305	IF	1:800
Anti-rabbit-488	Imm. Sciences	IS20014	IF	1:800
Anti-guinea pig-594	Mol. Probes	A11076	IF	1:800
Phosfo-Histone H2A.X-(Ser139)-Rb	Cell Signaling	9718	WB	1:1000